Journal of Materials Processing Technology, 28 (1991) 321-334
Elsevier

An experimental investigation into the stamping of elastic–plastic circular plates

L.C. Zhang

University Engineering Department, Cambridge CB2 1PZ, UK

T.X. Yu

Department of Mechanics, Peking University, Beijing 100871, China

(Received April 26, 1990; accepted in revised form January 10, 1991)

Industrial Summary

This paper reports the results of an experimental investigation into the deformation processes of circular plates pressed by cylindrical/hemi-spherical punches into conical dies, showing the variations of strain distribution, the development of deformation, the relationship between wrinkling loads and plate/punch dimensions, the springback, the wrinkling modes corresponding to critical loads and their effects on subsequent forming processes, and so on. Finally, the paper presents some useful information for manufacturing engineers on the designing of forming tools for sheet metals.

Notation

A contact area between a plate and a hemi-spherical punch
b radius of a circular plate
E Young's modulus
h thickness of a plate
$\tilde{h}$ dimensionless plate-thickness, defined as $hE^{1/2}/(2bY^{1/2})$
K_r residual radial curvature
P punch load
P_c^* dimensionless critical wrinkling load of plates pressed by cylindrical punches, defined as $2PE^{1/2}/(\pi Y^{3/2}h^2)$
P_s^* dimensionless critical wrinkling load of plates stamped by a hemi-spherical punch, defined as $PE^{1/2}\beta_s^{1/2}/(\pi bY^{3/2}h^{3/2})$
r radial coordinate
w_p punch displacement
Y yield stress
z vertical coordinate
β_c radius of a cylindrical punch

β_s radius of a hemi-spherical punch
ϵ_r radial strain
ϵ_θ circumferential strain
θ circumferential coordinate

1. Introduction

Investigation of sheet-metal forming has been the focus of attention of scientists and manufacturing engineers for over a century. As an important technology in sheet-metal forming, the stamping of sheet metals into dies of specific shape has been investigated by many researchers. It has been realised that in this kind of cold-forming operation, the following limiting phenomena are of primary importance:

(i) wrinkling of the sheet metal caused by compressive stresses;
(ii) tensile or shear failure of the workpiece;
(iii) springback during unloading; and
(iv) damage of forming tools, for example when the necessary forming load exceeds the ultimate/fatigue strength of a tool or causes its rapid wear.

However, thorough discussions of these phenomena related to the title problem have been few. Johnson and Singh [1] have pointed out that, according to the results of their experiments, the springback of a circular plate pressed by a hemi-spherical punch increases as the plate radius decreases. Yu, Johnson and Stronge [2] and Stronge, Sutcliffe and Yu [3] have investigated the same problem experimentally and analytically, their experimental results showing that the number of circumferential wrinkling waves of the workpieces ranges from four to six, whilst their analytical predictions indicate the development of two waves which correspond to critical wrinkling. In an experimental study of the stamping of soft and hard aluminum plates between a hemi-spherical punch and die, Yasuhisa, Kawada and Tozawa [4] found that the wrinkling loads for thinner (or harder) plates were lower than those for thicker (or softer) plates.

The present paper reports the results of a thorough investigation into the processes of deformation of circular plates pressed by cylindrical/hemi-spherical punches into conical dies (Fig. 1), which involve the primary problems of cold forming operations stated above. Tests of more than sixty specimens show, systematically, the variation of the distribution of the components of strain, the punch load–punch displacement curves, the relationship between wrinkling loads and the plate/punch dimensions, the springback, the wrinkling modes corresponding to critical loads and their effects on subsequent forming process, and so on. However, the present aim is to reveal mechanisms of deformation from the mechanics points-of-view, rather than to explore a real cup-forming process.

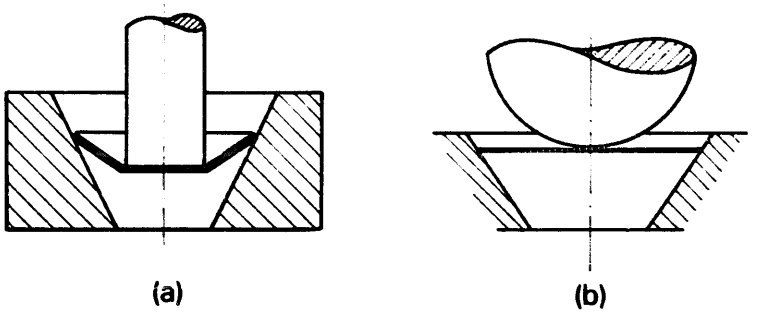

Fig. 1. Schematic diagram of the forming process: (a) using a cylindrical punch; (b) using a hemispherical punch.

2. Description of the experiments

A set of special precision tools to carry out the stamping process was manufactured (Fig. 2(a)). Initially, the plate (10) rests horizontally in the conical die (9) with its periphery in continuous contact, the punch (8), plate and die being set concentrically. The load from a universal testing machine is applied to the plate vertically through the press column (1) and the punch. The surface-strain components, ϵ_r and ϵ_θ, were transmitted by strain gauges (11) which were glued onto the upper and lower surfaces of the plate in advance, in the radial and circumferential directions. The resistance ring (2) and the terminal (7) constitute an angle sensor, combining with the vertical displacement sensor (3) fixed to the disk chuck (5) to detect the occurrence of wrinkling waves and to draw the exact shape of the wrinkling mode with the aid of an X–Y recorder: the whole frame composed of the disc chuck (5), the columns (6) and the bottom wheel (16) can rotate around the central axis of the instrument concentrically. The dial indicator (4) is used to measure the rigid-body displacement of the plate, the central deflection of which is recorded by the combination of the displacement sensor (15) and the guide-bar (13). The curve relating punch load and punch displacement is drawn directly on an X–Y recorder attached to the testing machine. Punches and dies of various dimensions and shapes were employed for various cases. The cone angle of the dies is 40 degrees. The punch descends at the low rate of 3 mm/min. No lubricant was used. Tests with same conditions of loading and specimen dimensions were repeated three to five times. When a hemi-spherical punch was used, the contact area between the punch surface and the plate was recorded by "press marks", which were obtained by putting a piece of carbon paper into the gap, prior to the carrying out of the test.

An electronic universal testing machine of type DSS-25^T was used in the experiments, its load range being from 1 kg to 25 t, with an attainable precision of $\pm 1\%$ and a minimum resolving power of 10 g.

The specimens were made of cold-rolled steel sheet of thicknesses 1.5 mm and 2.0 mm. As an example, Fig. 3 shows the stress–strain curves in the direc-

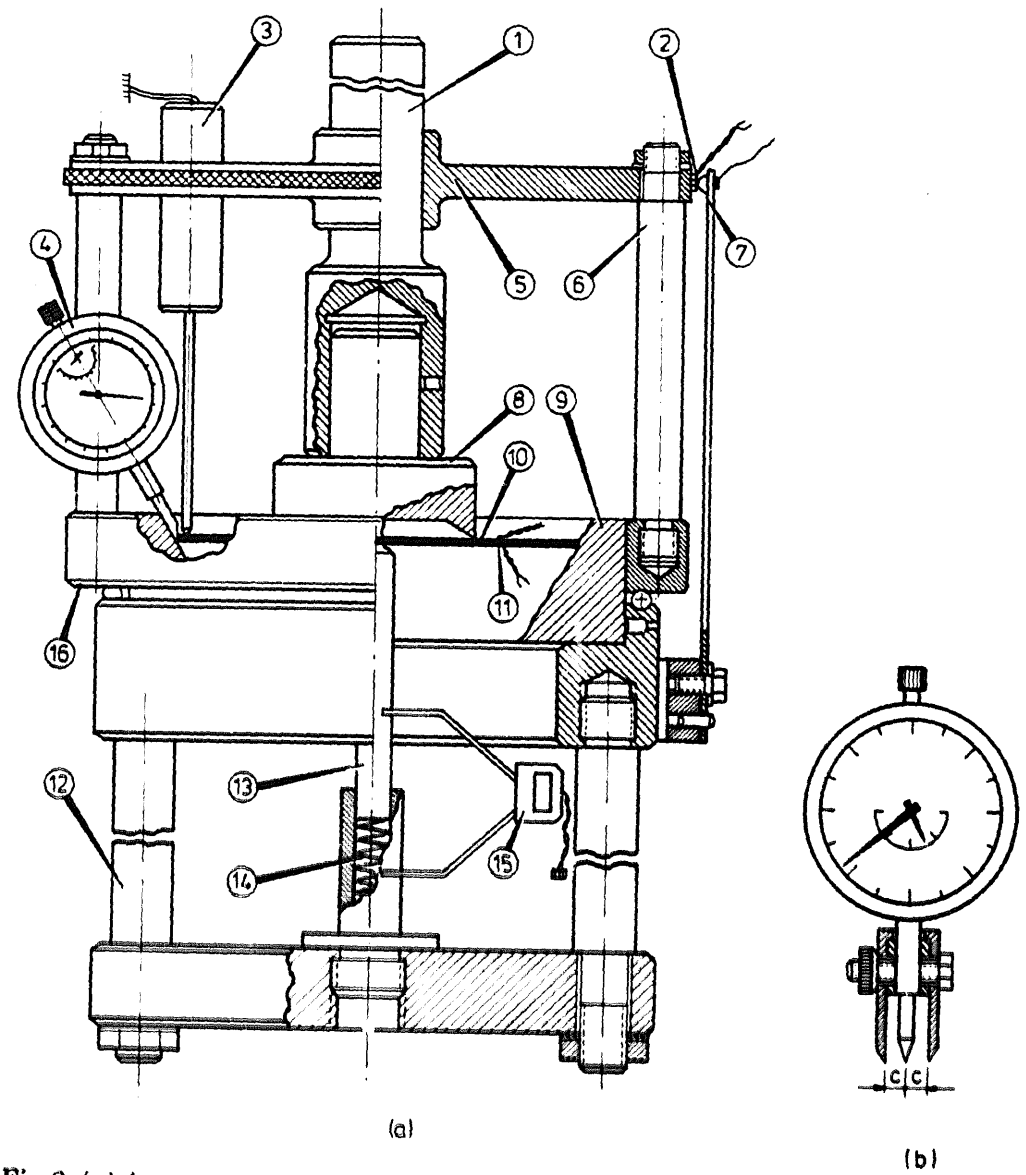

Fig. 2. (a) A cut-away view of the experimental tool; (b) the spherometer used to measure residual radial curvature.

tions of 0°, 45° and 90° with respect to the rolling direction of the sheet. It is evident that the in-plane anisotropy of the sheets is quite slight.

For the sake of convenience, the following notation is used to distinguish each workpiece:

A_1-A_2-A_3A_4

where A_1 is the diameter of the workpiece, A_2 is the thickness of the workpiece, A_3 is the kind of punch (C for cylindrical and S for hemi-spherical punches) and A_4 is the diameter of the punch applied. For example, 150-2.0-C45 stands

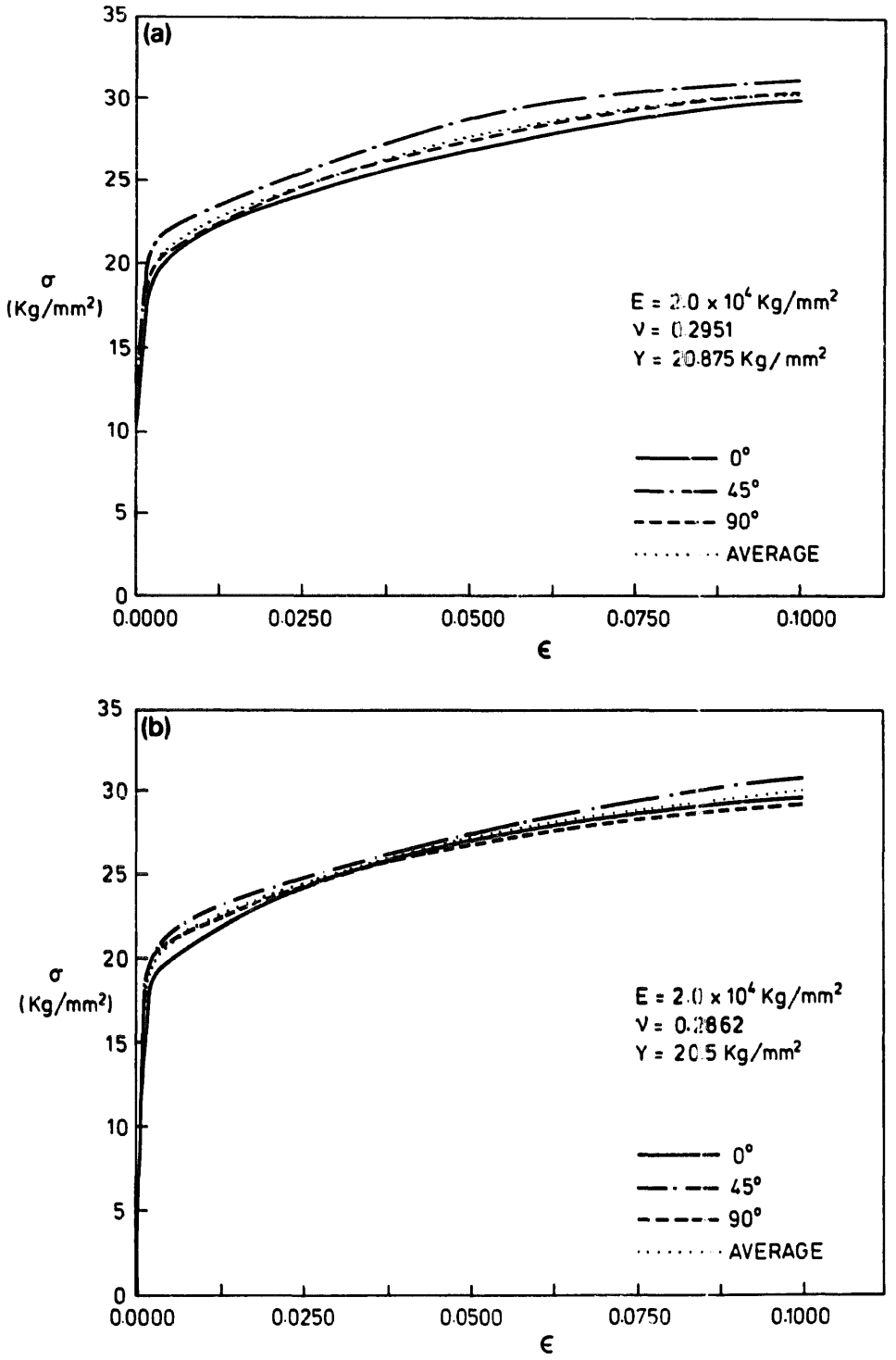

Fig. 3. Stress-strain curves of the cold-rolled steel sheets: (a) thickness 1.5 mm; (b) thickness 2.0 mm. (1 kg/mm^2=9.81 MPa).

for a workpiece of diameter 150 mm and thickness 2.0 mm, pressed by a cylindrical punch of diameter 45 mm.

After stamping, the final shapes and residual curvatures of the workpieces were measured by a spherometer, shown in Fig. 2(b). Using the meter readings, the local average curvatures were calculated by the finite-difference method.

3. Results and discussions

3.1. Strain distributions

Figure 4 shows the variation of the distribution of the strain components of workpiece 150-1.5-C45 with increase of external load: similar results were obtained for other specimens. The figure indicates that the circumferential strain, ϵ_θ, forms a wide band of negative value near to the periphery of the plate. Hence, the plate element within this negative ϵ_θ band must be subjected to a circumferential compressive internal force, which is the essential factor in the development of wrinkling. As expected, the radial strain, ϵ_r, at $z=h/2$ is always positive, see Fig. 4(c), but the positive values of ϵ_r appearing on part of the upper surface $z=-h/2$ is unexpected. However, it is noted that the plate was supported by the conical die at its periphery of $z=h/2$ and hence a negative bending moment acted on the plate boundary as the supporting was assumed to be moved to its mid-plane according to the equivalent principle of equilibrium, see Fig. 5: thus the value of ϵ_r on $z=-h/2$ should indeed be positive near to the periphery.

3.2. Springback and wrinkling

The punch load–punch displacement curves (P–w_p curves) of 150-2.0-C45 and 150-2.0-C65, shown in Fig. 6, indicate that the springback of a plate during unloading decreases with increase of deformation (or external load, or deflection). It follows from the comparison of the present results with that of the stamping of a strip into a cylindrical die [5] that the amount of springback of a doubly-curved shell during unloading (as with the present specimens) is far less than that of a singly-curved shell, the reason being that the load-bearing capacity of the former is much better than that of the latter. Figure 6 reveals also that there exist very evident slope changes in the P–w_p curves as wrinkling or post-wrinkling occurs.

As shown in Fig. 7, non-dimensional critical wrinkling loads P_c^* and P_s^* vary monotonously with dimensionless plate thickness $\tilde{h}$, where

$$\tilde{h}=hE^{1/2}/(2bY^{1/2})$$

$$P_c^*=2PE^{1/2}/(\pi Y^{3/2}h^2)$$

$$P_s^*=PE^{1/2}\beta_s^{1/2}/(\pi bY^{3/2}h^{3/2})$$

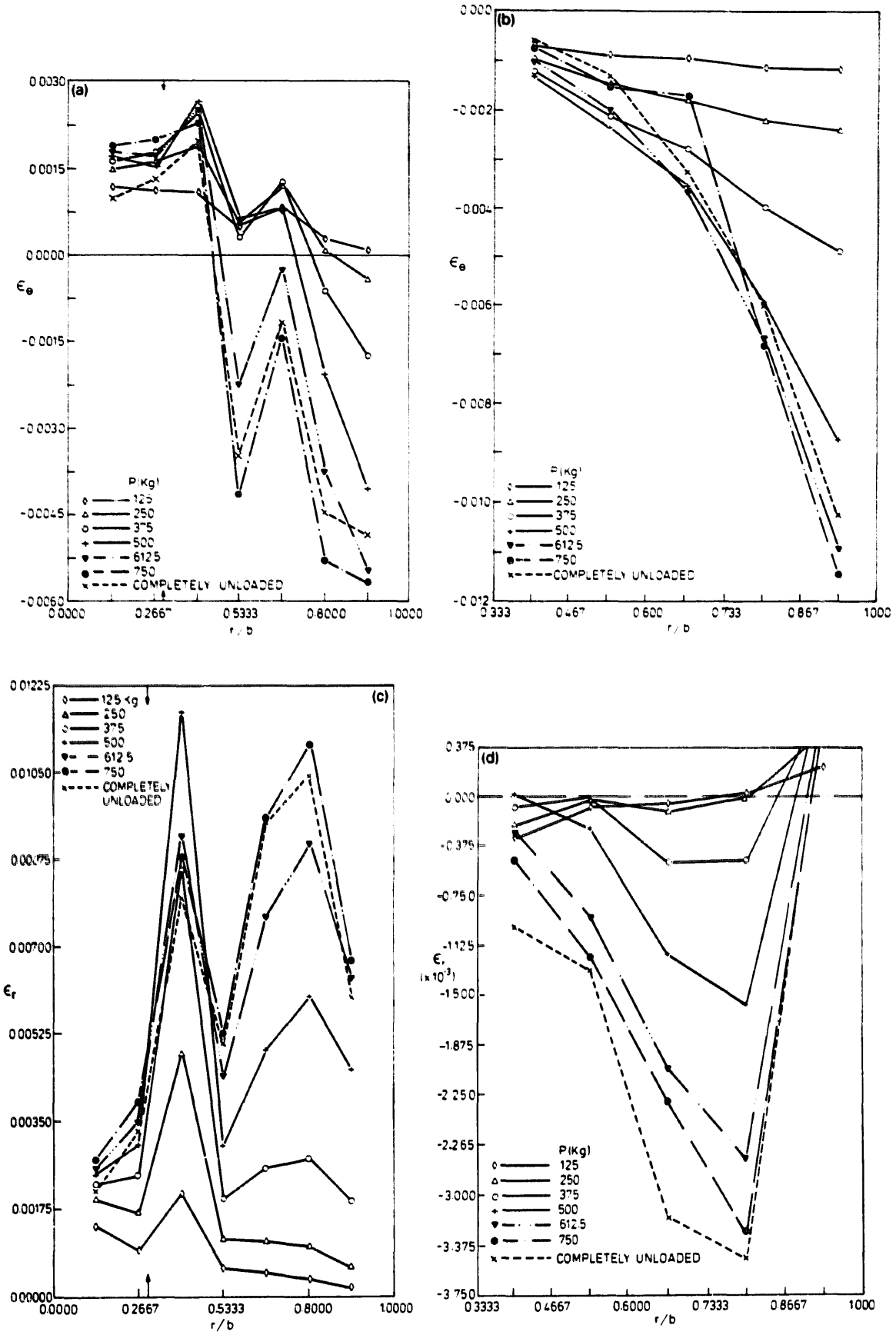

Fig. 4. Strain distribution of specimen 150-1.5-C45: (a) ϵ_θ on $z=-h/2$; (b) ϵ_θ on $z=h/2$; (c) ϵ_r on $z=h/2$; (d) ϵ_r on $z=-h/2$.

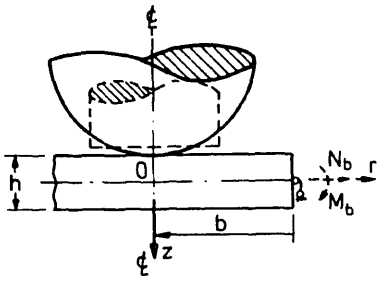

Fig. 5. Equivalent boundary-conditions.

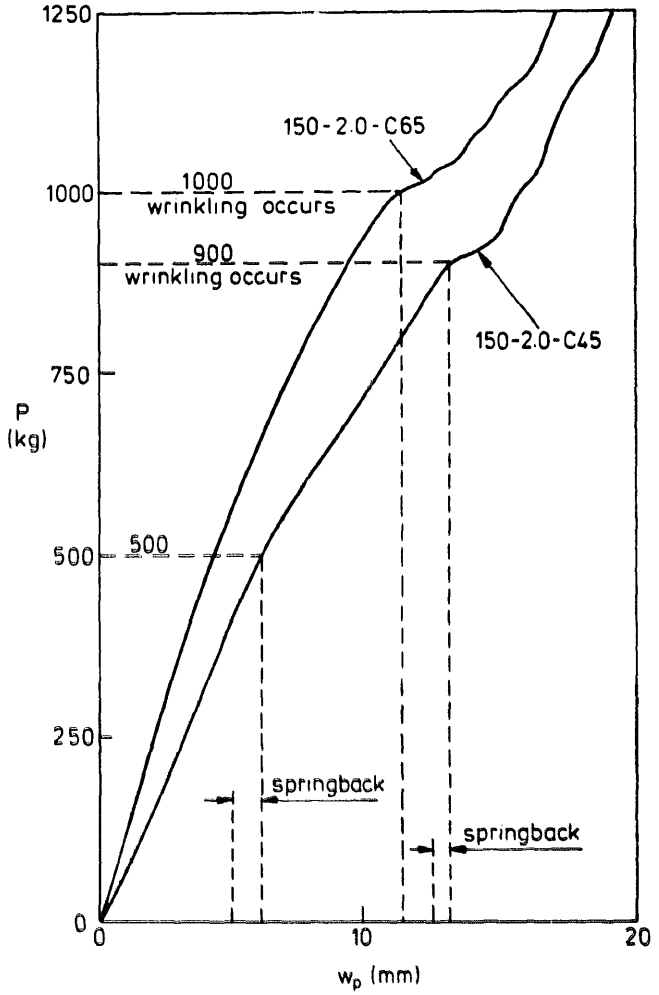

Fig. 6. Curves of punch load vs. punch displacement.

Value P_c^* represents the critical wrinkling load of plate stamped by a cylindrical punch whilst value P_s^* is that of a plate pressed by a hemi-spherical punch of radius β_s. These non-dimensional groups were obtained by dimensional analysis [7]. The results show that P_s^* is much more sensitive to $\tilde{h}$ than is P_c^* as $\tilde{h}$ becomes small. Although the relationship between P_s^* and $\tilde{h}$ is quite

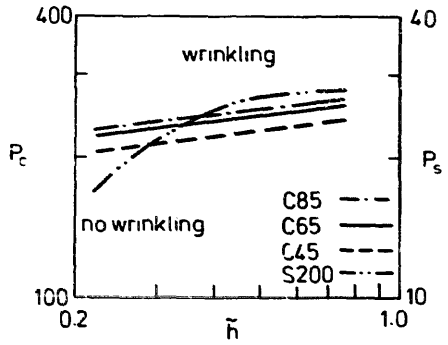

Fig. 7. Dependence of the critical wrinkling load upon the dimensionless plate-thickness.

complicated, P_c^* can be fitted approximately by a power function of $\tilde{h}$. Moreover, the figure indicates that variation of the radius of the cylindrical punches, β_c, only shifts the P_c^* curve. Hence, a pithy equation to predict the critical wrinkling load can be expressed as

$$P_c^* = C_1(\tilde{h}^{3/20})\,[(\beta_c/b)^{1/5}] \tag{1}$$

where C_1 is a constant and the exponents 3/20 and 1/5 are obtained from the experimental results.

3.3. *Wrinkling mode corresponding to the critical load*

Whether for specimens pressed by cylindrical punches or for those pressed by the hemi-spherical punch, wrinkling modes corresponding to critical wrinkling loads were in the form of four waves. Figures 8(a) and (b) are representative photographs of the specimens (in this case 150-1.5-C45 and 150-1.5-S200) after their first wrinkling, the circumferential wave shapes being as shown in Fig. 8(c). The process of the change of deformation pattern from an axisymmetric to an asymmetric one is shown directly by the press marks, as those in Fig. 9 (here taking 150-2.0-S200 as representative), which trace clearly the evolution of the contact area between the plate and the hemi-spherical punch.

An exceptional example which leads to a three-wave wrinkling mode and then doubles to a six-wave mode was found in the repeated test of 120-1.5-S200, where the three-wave mode corresponded to a wrinkling load $P=612.5$ kg. However, a four-wave mode of the other specimens only required 562.5 kg to wrinkling. Furthermore, the central displacement of the former at wrinkling was 14.17 mm, whilst that of the latter was 12.20 mm. Hence, this exceptional example does not negate the above-mentioned general conclusion that the four-wave mode corresponds to critical loads.

3.4. Load–contact area relationship

During axisymmetric deformation of plates stamped by the hemi-spherical punch, the relationship between punch load P and contact area A was found to be

$$P \approx C_2 A \tag{2}$$

where C_2 is a constant for a plate with specific dimensions.

3.5. Effect of initial imperfections

Although the specimens were processed meticulously, small initial imperfections were difficult to avoid. However, the experiments showed that the curves of punch load against punch displacement from the repeated tests agreed very well (including wrinkling loads and their corresponding wrinkling modes). It can be concluded, therefore, that the wrinkling of plates stamped into conical

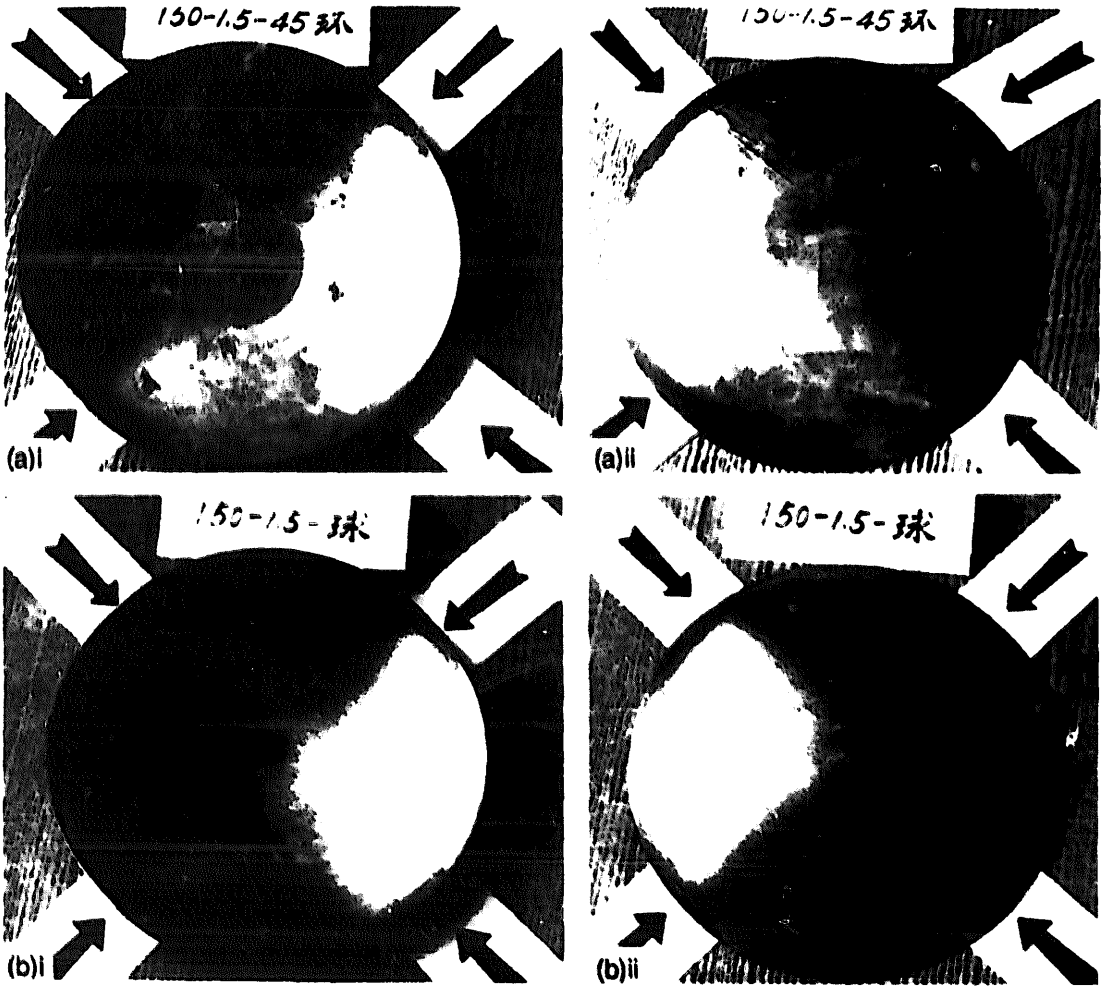

Fig. 8. Wrinkling modes: (a) 150-1.5-C45 (i) concave-side view, (ii) convex-side view; (b) 150-1.5-S200 (i) concave-side view, (ii) convex-side view.

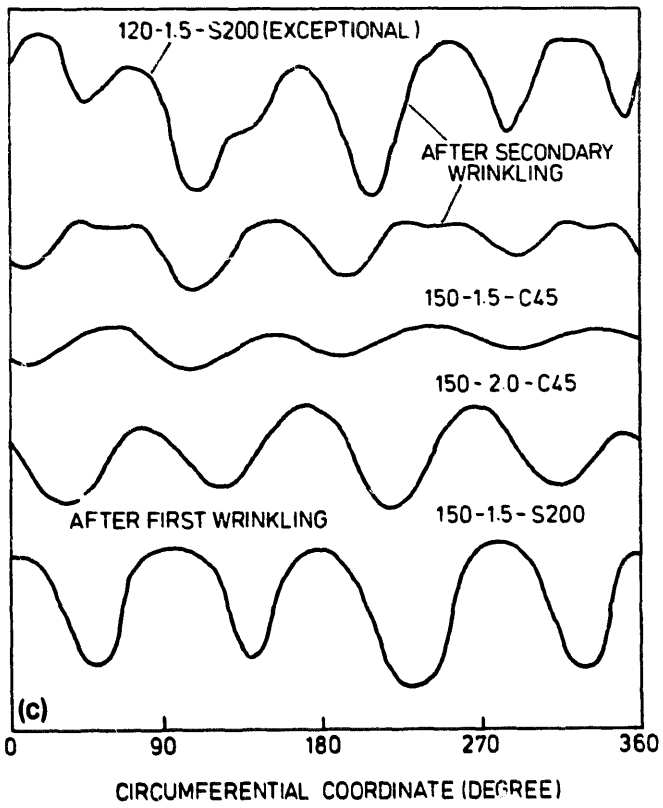

Fig. 8. Wrinkling modes: (c) circumferential shapes.

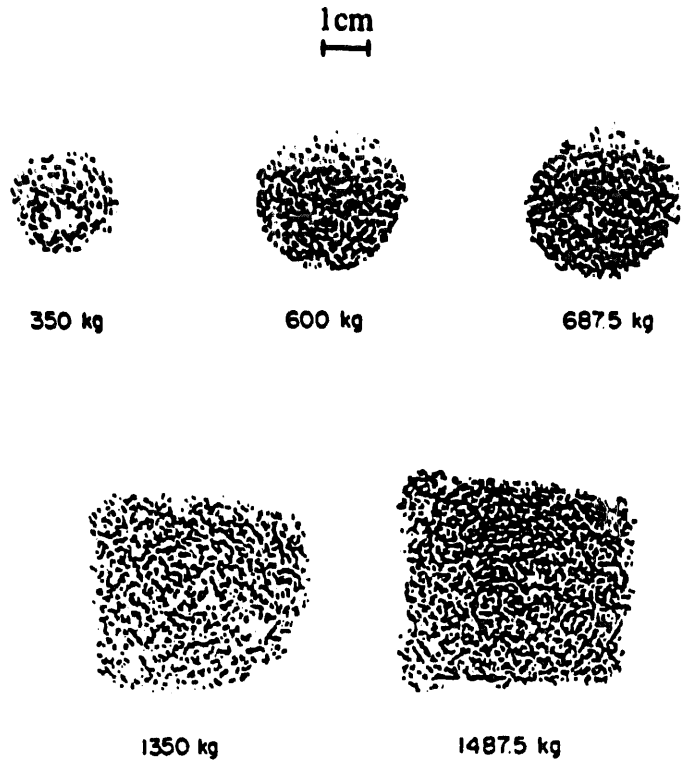

Fig. 9. Press marks on 150-1.5-S200.

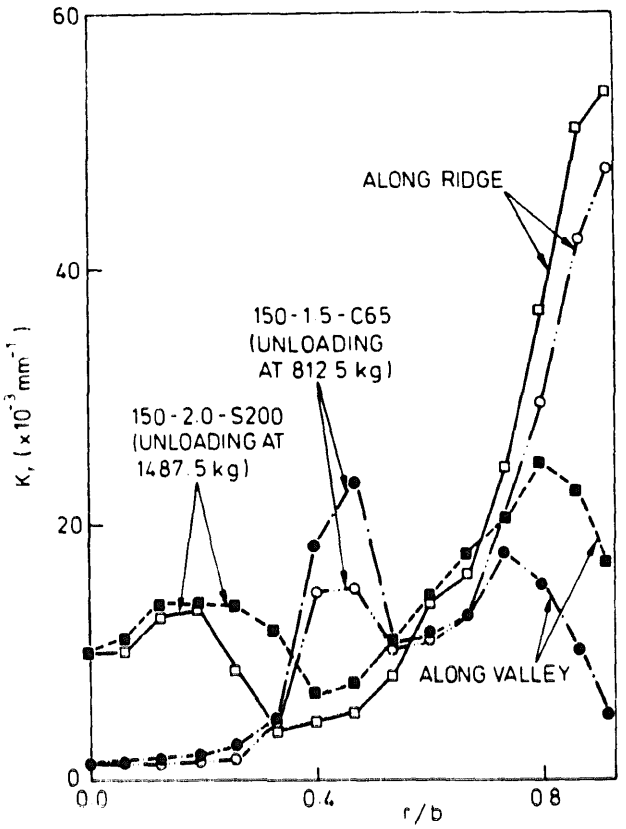

Fig. 10. The residual radial curvatures after first wrinkling (after unloading).

dies by cylindrical/hemi-spherical punches is insensitive to their small initial imperfections.

3.6. Doubling of wrinkling waves

The doubling of wrinkling waves, or secondary wrinkling, was first pointed out by Senior and was afterward described in some detail by Johnson and Mellor [6] and Yu, Johnson and Stronge [2]. However, all of these authors thought that it was similar to that in the deep-drawing process when a blank-holder is used, and accordingly that the wave doubling of a plate pressed by a hemispherical punch is due to the contact between the punch and the ridges of the wrinkling wave. However, the present experiments have shown that this is not always the case, since in some of the tests the doubling occurred before the punch made contact with the wave ridges. The doubling phenomenon of the wave for 150-1.4-C45 shown in Fig. 8(c), is a good example of such, where the use of a cylindrical punch ensured that no contact with the wave ridge might take place.

3.7. Radial curvatures

Figure 10 illustrates the radial residual curvatures, K_r, for specimens 150-2.0-S200 and 150-1.5-C65 after their first wrinkling. It was found that the ra-

dial wave peaks of the wrinkling mode appeared inside the periphery of the specimen: the phenomenon can be observed also directly from the photographs shown in Fig. 8(a) and (b). Obviously, this is an unfavourable feature for the subsequent stages of deformation of the plate. For example, in the forming process of a shallow spherical shell pressed by a hemi-spherical punch and die, if the wrinkling mode as described above appears, the ironing of waves has to overcome more resistance. As a result, a large press is needed, the service life of the die is shortened and the workpiece may fracture at its periphery. Therefore, manufacturing engineers should try to avoid the appearance of such wrinkling waves. According to the present results, the authors suggest that one of the means to avoid this situation is to control the height to which the shell is deformed in a single operation.

3.8. An approximate analytical model

Figures 4, 8(a) and 10 indicate that the deformation of specimens pressed by cylindrical punches is concentrated mainly in the area outside the punch. Therefore, a simple approximate analytical model proposed for engineers to evaluate wrinkling loads, which will not yield results far from reality, is as follows:

"The plate element inside the circle of the end profile of a cylindrical punch is considered as a rigid one: deformation occurs only on the portion outside the circle and the circumferential wrinkling mode is in the shape of a four-wave sine/cosine curve."

4. Conclusions

(1) For plates pressed by hemi-spherical and cylindrical punches, a four-wave mode first appears at critical wrinkling loads. Moreover, this mode bears no relation to the diameter-to-thickness ratio of the plates.

(2) The wrinkling loads are monotonous functions of dimensionless plate thickness $\tilde{h}$. The relation between P_s^* and $\tilde{h}$ can be described by a single curve whereas that for P_c^* can be determined approximately by the use of eqn. (1). Increase in the ratio of the diameter of the cylindrical punch to that of the plate improves the formability, that is, it delays the occurrence of wrinkling.

(3) Springback decreases with increase of deformation.

(4) The occurrence of wrinkling is accompanied by an evident slope change in the load–deformation curve.

(5) The wrinkling is insensitive to small initial imperfections in the workpieces.

(6) The doubling of wrinkling waves may occur before the punch makes

contact with the wave ridges: this phenomenon should be noted by tool designers.

(7) Punch loads before wrinkling are approximately linear functions of the contact area between the hemi-spherical punch and the plates.

References

1 W. Johnson and A.N. Singh, Springback in circular blanks, *Metallurgia* (May 1980) 275-280.
2 T.X. Yu, W. Johnson and W.J. Stronge, Stamping and springback of circular plates deformed in hemispherical dies, *Int. J. Mech. Sci.*, 26 (1984) 131-148.
3 W.J. Stronge, M.P.F. Sutcliffe and T.X. Yu, Wrinkling of elasto-plastic circular plates during stamping, *Exp. Mech.*, (December 1986) 345-353.
4 H. Yasuhisa, H. Kayada and Y. Tozawa, Forming force in spherical forming of circular plates, *J. Jpn. Soc. Technol. Plast.*, 22 (1981) 1223-1229.
5 T.X. Yu and L.C. Zhang, Numerical analysis of springback of strips after elasto-plastic bending and torsion, *Chin. J. Appl. Mech.*, 4 (1987) 19-26.
6 W. Johnson and P.B. Mellor, *Engineering Plasticity*, Van Nostrad Reinhold, London, 1973.
7 L.I. Sedov, *Similarity and Dimensional Methods in Mechanics*, Academic Press, New York, 1959.